

# On becoming a parasite: evaluating the role of wall oxidases in parasitic plant development

Dongjin Kim, Remigiusz Kocz, Laural Boone, W John Keyes and David G Lynn

**Background:** The temporal and spatial control of the transition from vegetative to parasitic growth is critical to any parasite, but is essential to the sessile parasitic plants. It has been proposed that this transition in *Striga* spp. is controlled simply by an exuded oxidase that converts host cell-surface phenols into benzoquinones which act as developmental signals that mediate the transition. An understanding of this mechanism may identify the critical molecular events that made possible the evolution of parasitism in plants.

**Results:** PoxA and PoxB are identified as the only apoplastic phenol oxidases in *Striga asiatica* seedlings, and the genes encoding them have been cloned and sequenced. These peroxidase enzymes are capable of oxidizing the 60 known inducing phenols into a small set of benzoquinones, and it is these quinones that induce parasitic development. Analysis of the reaction requirements and comparisons to host enzymes, however, lead us to argue that PoxA and PoxB are not necessary for host recognition.

**Conclusions:** A new model is proposed where constitutive production of an activated oxygen species (in the case of *Striga*,  $H_2O_2$ ) mediates host recognition. This strategy would allow a parasite to exploit abundant host enzymes to produce the diffusible recognition signals by converting a standard host defense into a parasitic offense.

## Introduction

One percent of all known flowering plants exploit parasitic associations with other angiosperms [1,2]. This parasitism is broadly distributed, with species across at least 16 families in habitats that range from the poles to the dry and humid tropics and in annuals and perennials in the form of trees, shrubs, vines, or herbs [3]. Such a broad and diverse distribution has suggested that the parasitic strategy was repeatedly discovered throughout angiosperm evolution [4].

Searcy and MacInnis [5,6] first proposed three general developmental phases for the molecular evolution of the parasitic plants. The first phase involved the development of the specialized organ that forms the physiological bridge to the host — the haustorium. The second and third phases involved specialization and adaptation of the parasite to the host. There is significant evidence in support of the idea that the parasite loses both biochemical pathways and morphological structures that become redundant upon attachment to the host [7–11], and for the accrual of more complex adaptations specific to an obligate parasite, such as host specialization [1,12–14] and mechanisms which overcome host defenses [15–18]. In contrast, less is known about the development of the host attachment organ. There are differences in anatomical features of mature haustoria across the parasitic plants, although there appear to be common elements in the early initiation events [1,18].

Lateral haustoria in the rhinanthoid Scrophulariaceae are initiated by early rounds of cell division and radial swelling in the pericycle and inner cortex layers of the root to give rise to the haustorial primordia. In the obligate hemi-parasite *Striga asiatica*, which can survive for only 5 days without host attachment, a transformation of the terminal root meristem occurs: cells in the root primordia stop dividing and radial swelling occurs just distal to the root tip, ultimately giving rise to the pre-attachment organ [18]. Both processes are very rapid (development of the haustorium is complete within 12–16 h), and are tightly coupled to host chemistry [12,18,19]. The same host recognition compound or xenognosin, 2,6-dimethoxy-*p*-benzoquinone (DMBQ), was identified as a natural signal that was necessary and sufficient for induction of both lateral and terminal haustoria in several of the Scrophulariaceae [12,20].

Prior to the discovery of DMBQ, a diverse array of simple phenols had been found to induce haustorial development in the Scrophulariaceae [12,19]. The discovery of DMBQ came from the observation that host cell wall fragments removed from sorghum root surfaces were found to induce haustorial development in *S. asiatica* [19]. During the incubation DMBQ accumulated, and when the concentration reached  $10^{-6}$  M, haustorial development was induced. Syringic acid, used as a model cell wall phenolic precursor, was oxidized to DMBQ by *S. asiatica* seedlings

Address: Searle Chemistry Laboratory, The University of Chicago, Chicago, IL 60637, USA.

Correspondence: David G Lynn  
E-mail: d-lynn@uchicago.edu

**Key words:** active oxygen species, haustoria development, host recognition, parasite evolution, parasitic plants, peroxidases, *Striga asiatica*, xenognosis

Received: 23 October 1997  
Revisions requested: 26 November 1997  
Revisions received: 12 January 1998  
Accepted: 13 January 1998

Published: 15 February 1998

Chemistry & Biology February 1998, 5:103–117  
<http://biomednet.com/elecref/1074552100500103>

© Current Biology Ltd ISSN 1074-5521

and induced haustoria only when the quinone concentration reached the micromolar minimal threshold. These results suggested that a parasite enzyme was required to oxidatively liberate the inducing signal, sorghum xenonin for *Striga haustoria* (SXSh), from the host cell surface [12,19]. Consistent with that model, extensive washing of *S. asiatica* seedlings prior to placing them on host roots prevented haustorial development. This inhibition of haustorial development was reversed, however, when a solution of *Pyricularia oryzae* laccase (benzenediol:O<sub>2</sub> oxidoreductase; EC 1.10.3.2) was added to these washed seedlings while on the host surface, presumably because the enzyme reconstituted the oxidizing activity.

The model of a parasite phenol oxidase mediating host detection was appealingly simple and motivated the investigation reported here. We report the isolation of two apoplastic oxidases from *S. asiatica*, and the cloning and sequencing of their encoding genes. These oxidases account for the wide range of structural variability acceptable for the xenonin signal, as they catalyze the oxidation of diverse phenols to a common benzoquinone. We argue, however, that these parasite enzymes need play no role in host recognition; rather, the parasite can enlist homologous host enzymes for that task.

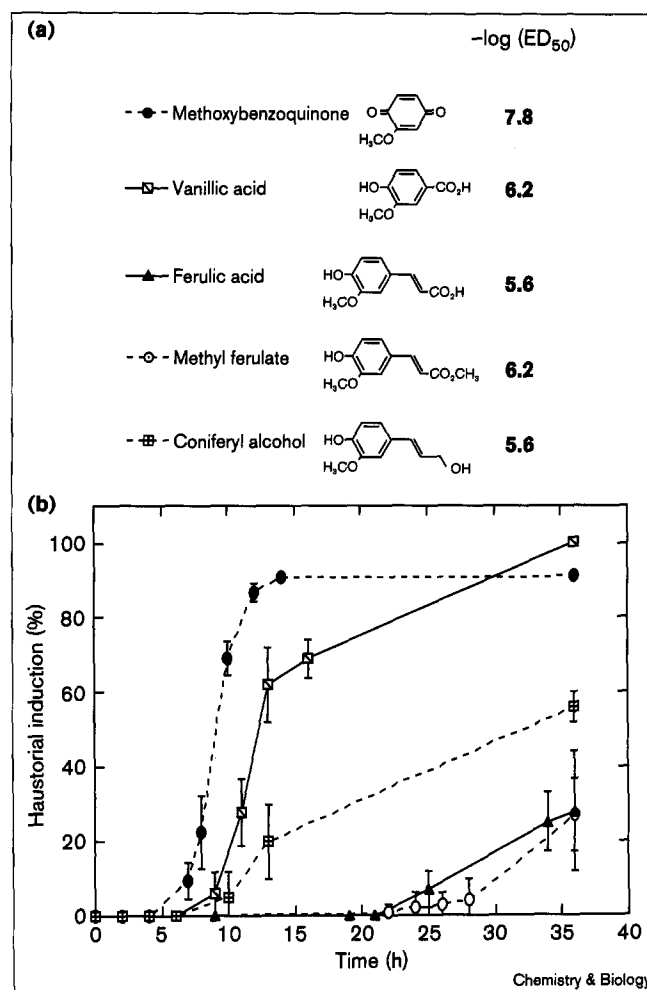
## Results

### Source of SXSh

Root surface abrasion experiments had previously implicated the plant cell wall as the source of SXSh [12,19]. Cell walls were isolated from sorghum roots and this fraction induced, depending on the isolate, 20–40% of the *S. asiatica* seedlings to develop haustorial primordia. Further fractionation of the walls demonstrated that all the haustorial-inducing activity was associated with the pectin-containing fraction. After saponification of this fraction, all the inducing activity partitioned from H<sub>2</sub>O into Et<sub>2</sub>O. Both the organic soluble fraction and the initial pectic fraction required a 30–40 h incubation time for half-maximal haustorial induction, consistent with phenyl propanoid esters in the pectic fraction being responsible for the induction.

Plant cell walls are known to contain specific phenyl propanoid-derived phenolics that differ in degree of methoxylation [21]. Oxidation of the aryl-C $\alpha$  bond of these phenyl propanoids would give methoxybenzoquinone, 2,6-dimethoxybenzoquinone, and the unsubstituted *p*-benzoquinones, all of which have been shown to be active haustorial inducers [22]. More than 60 other synthetic phenolics were further investigated [23,24], and those that contained the appropriate substitution pattern to be oxidized to an active quinone induced haustoria. These active phenolics, however, required a concentration that was at least an order of magnitude higher than the similarly substituted quinones themselves (Figure 1a). For example, the half-maximal concentration for the monomethoxy

Figure 1



Induction of haustorial development in *S. asiatica* seedlings. (a) Dependence on concentration. (b) Dependence on time at  $10^{-6}$  M inducer.

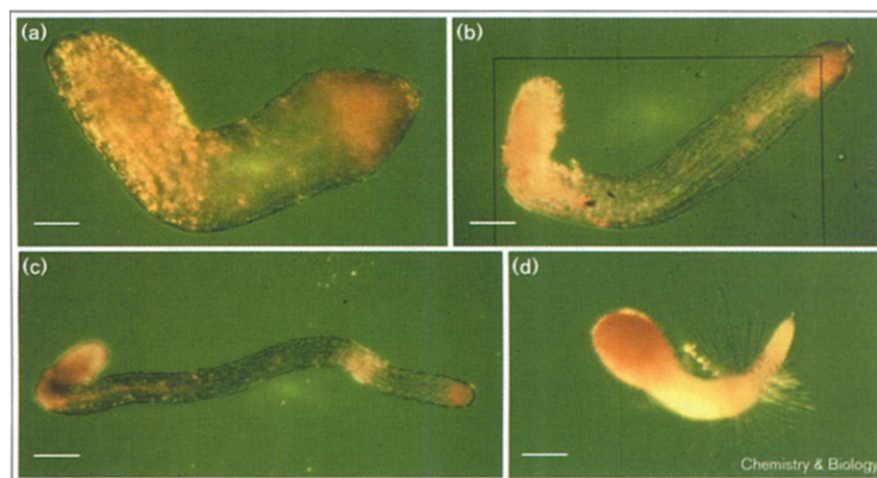
phenols varies between  $10^{-5.6}$  M and  $10^{-6.2}$  M whereas monomethoxybenzoquinone shows half-maximal activity at  $10^{-7.8}$  M. The seedling exposure time required for haustorial induction by the active phenols was also consistently longer than that of the analogous quinones. Compounds with an oxygenated carbon *para* to the phenol hydroxyl group, such as vanillic acid, required relatively short exposure times. The phenyl propanoids, ferulic acid and methyl ferulate, required exposure times of 30–40 h, similar to the pectic fractions (Figure 1b). A similar substrate dependence has been reported for the rate of peroxidase-catalyzed oxidations of phenyl propanoids [25,26].

### Histochemical staining

The broad structural range of the active phenols suggested that chromophoric substrates could be used to localize the oxidase(s). Both syringaldazine and pyrogallol identified oxidase activity concentrated at the meristematic root tip

**Figure 2**

Histochemical staining of *S. asiatica* and *Arabidopsis thaliana* seedlings. (a) One day-old *Striga* seedling. (b) Two day-old *Striga* seedling. (c) Three day-old *Striga* seedling. (d) Two day-old *Arabidopsis* seedling. Scale bars: (a) 40  $\mu\text{m}$ ; (b) 80  $\mu\text{m}$ ; (c) 150  $\mu\text{m}$ ; (d) 250  $\mu\text{m}$ .



of one, two and three day-old *S. asiatica* seedlings (Figure 2a–c). The reddish coloration from the pyrogallol took several seconds to develop and was most strongly detected in the presence of added  $\text{H}_2\text{O}_2$ . Several other monocot and dicot seedlings were also screened with these substrates and the 2 day-old *Arabidopsis* seedling shown in Figure 2d is typical. The *Arabidopsis* root hair zone had very strong oxidase activity, much stronger than *Striga*, and the color developed immediately upon addition of  $\text{H}_2\text{O}_2$ , but not at all in the absence of the  $\text{H}_2\text{O}_2$  co-substrate. Peroxidase activity has been shown to be localized in the walls of the root cap and epidermal cells in older wheat seedlings [27]. *S. asiatica*, however, has no root cap and no root hairs; only the walls of the root meristem cells appeared to accumulate the stain. Some stain did develop around the site of emergence from the seed coat, which might be attributed to transient wound-induced peroxidase expression. Removal of the seed coat (Figure 2a–c) revealed the orange-pigmented embryo that did not accumulate stain from either substrate.

#### Extraction of oxidases bound to the cell wall

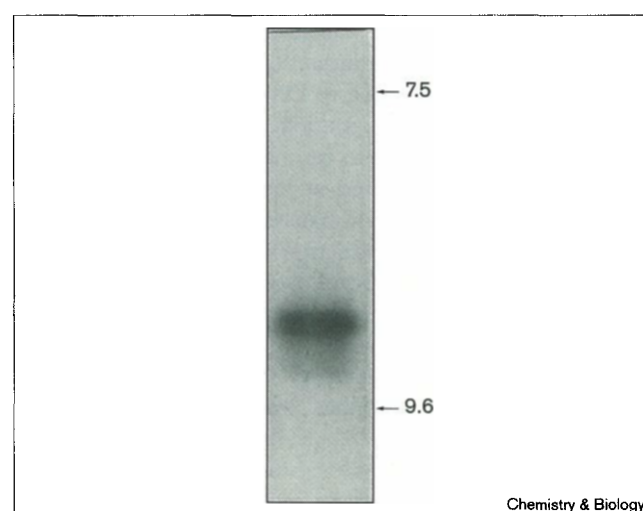
The identified oxidase activity was removed by extensive washing of the *S. asiatica* seedlings as previously reported [12,19]. Because the histochemical staining suggested that the oxidase activity was concentrated within the cell walls, an isolated cell wall fraction was extracted with 1M NaCl, using the methods of Kay and Basile [28] to enrich the activity. When the extract was desalted and analyzed by isoelectrofocusing gel electrophoresis, two diffuse basic peroxidase bands that depended on added  $\text{H}_2\text{O}_2$  were typically detected, both with pI's of ~9 (Figure 3).

The wall extract, under the conditions used in the whole seedling experiments — with the exception that  $\text{H}_2\text{O}_2$  was not added — catalyzed the oxidative cleavage of the

aryl-C $\alpha$  bond of phenols. At pH 5.5, the half-life of syringic acid was shorter, 4 h as compared to 27 h, and the conversion of syringic acid to DMBQ was much higher, 17% as compared to 2%, than found with intact seedlings. The rate and yield increases *in vitro* may be attributed to higher oxidase concentration, an apparently greater stability of the quinones *in vitro*, and/or the greater availability of  $\text{H}_2\text{O}_2$ .

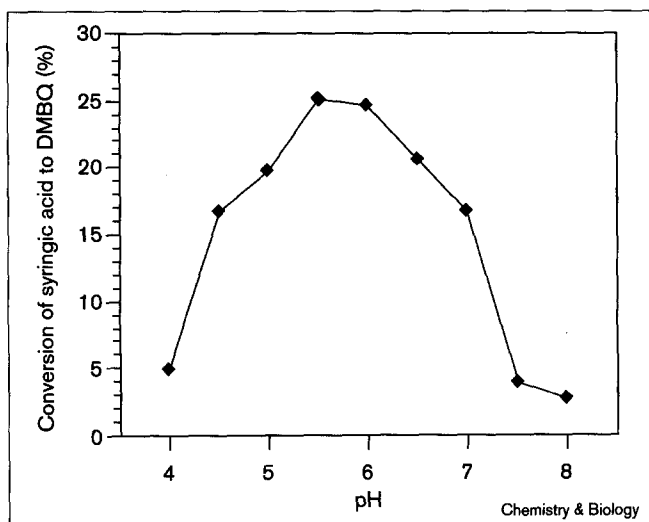
#### Dependence of haustorial induction on pH

We used several approaches to evaluate the involvement of the identified enzymatic activity in haustorial induction. Oxidase inhibitors, such as the peroxidase inhibitors  $\text{N}_3$  and

**Figure 3**

Isoelectrofocusing gel of *S. asiatica* cell wall proteins. The peroxidase activity on the gel was detected with a peroxidase assay solution, and the pI's of standard proteins are as marked.

Figure 4



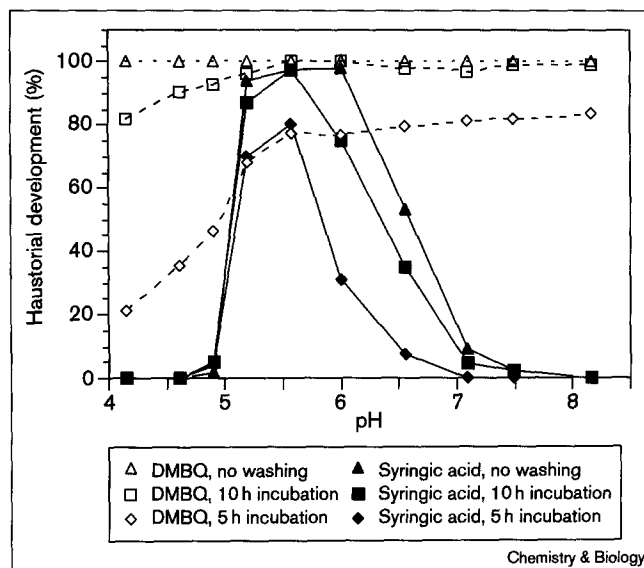
Dependence of the conversion of syringic acid to DMBQ *in vitro* on pH. The percent conversion was calculated from the ratio  $[\text{DMBQ}]/([\text{DMBQ}] + [\text{syringic acid}])$ , from a 4 h time point. The 4 h time point was chosen because the half-life of the syringic acid to DMBQ reaction is 4 h at pH 5.5.

CN, are generally metabolic toxins that interfere with haustorial development. The pH dependence of the oxidase activity proved most valuable in our analyses, however. Figure 4 shows the pH dependence of the conversion of syringic acid to DMBQ by the extracted oxidases. DMBQ was stable under the reaction conditions, and the conversion required the presence of  $\text{H}_2\text{O}_2$  throughout the explored pH range. The pH optima occurred between 5.5 and 6; at pH  $\leq 4$  and  $\geq 7.5$  there was no significant oxidation of syringic acid to DMBQ.

Figure 5 shows the pH-dependence of haustorial development. *S. asiatica* haustorial induction is independent of pH when seedlings are exposed to DMBQ for long periods of time ( $>10$  h). The time-dependence of quinone exposure, however, has been shown to be crucial [22,29], and longer exposure times are required at low pH. At pH 4.2, only 22% of the seedlings formed haustoria after a 5 h exposure to DMBQ, but at 10 h induction approached that of the unwashed control. The morphology of the haustoria was not significantly altered across this pH range (Figure 6c,d).

At pH 5.6, haustoria induced by syringic acid were morphologically indistinguishable from those induced by DMBQ. At pH 5.2, however, swelling and haustorial hairs form, but haustorial morphology was abnormal (Figure 6b). Below pH 5,  $10^{-4}$  M syringic acid was toxic to the seedlings (Figure 6a); the root tips showed a pronounced darkening and the seedlings were no longer viable even after syringic acid removal. Between pH 6 and 7, the longer the exposure time to the syringic acid, the higher

Figure 5



Dependence of haustorial induction with syringic acid and DMBQ on pH. *S. asiatica* seedlings (1.5 days old) were placed in 2 mM potassium phosphate buffer over a pH range of 4.0 to 8.5. The seedlings were incubated at 27°C with either  $10^{-4}$  M syringic acid or  $10^{-5}$  M DMBQ for 5 h or 10 h before being washed with three volumes of the designated buffer and further incubated with fresh buffer. Haustoria were counted and photographed after 2 days of incubation.

the percentage of haustorial induction, but beyond pH 7, few haustoria were induced.

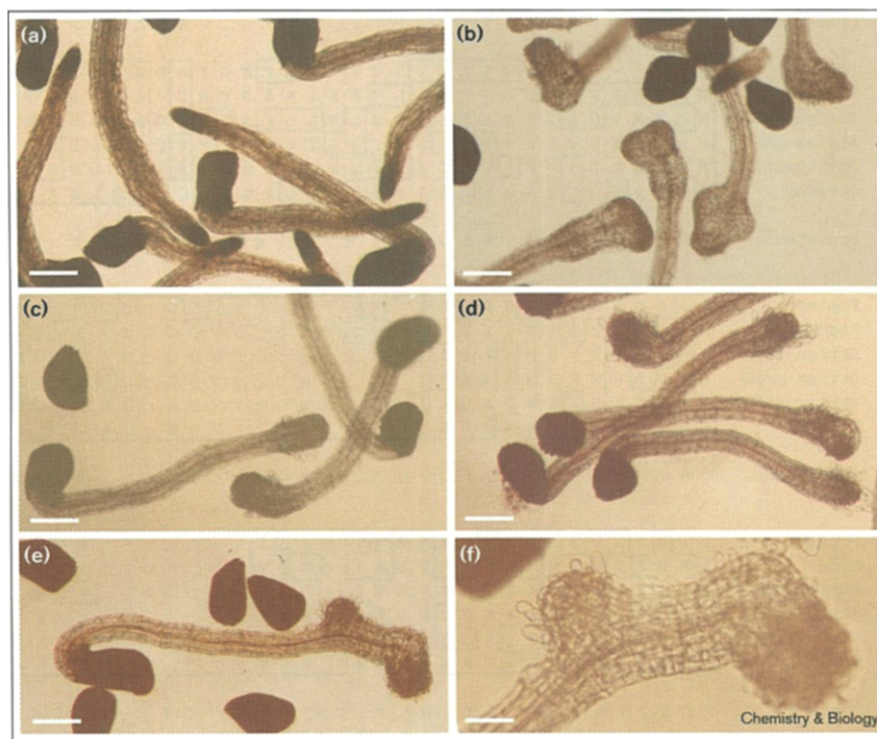
When syringic acid was not removed, many of the seedlings formed double haustoria (Figure 6e,f). Such double haustoria have been described in previous experiments [29] after multiple exposures to DMBQ. The exposure of seedlings to DMBQ for 6–10 h is sufficient to induce full haustorial development. Following removal of DMBQ, the seedlings were found to develop a new root primordium, one that was subsequently responsive to haustorial induction by DMBQ. Seedlings exposed to syringic acid for long periods of time were similar in appearance to these seedlings that saw multiple DMBQ exposures [29], as though the inducing signal had been removed to allow for meristem development and then reapplied.

#### The role of $\text{H}_2\text{O}_2$ in haustorial induction

There are several classes of oxidases. In order to determine what kind of oxidase was involved in *Striga* haustorial induction, we investigated the requirement of  $\text{H}_2\text{O}_2$  in the induction process. A distinguishing feature of peroxidases, in comparison to other phenol oxidases, is a dependence on  $\text{H}_2\text{O}_2$  as a co-substrate. An haustorial-induction model that involves conversion of phenols to benzoquinones, catalyzed by wall peroxidases would require the  $\text{H}_2\text{O}_2$  co-substrate to be supplied to the parasite apoplast. We therefore evaluated the requirement for  $\text{H}_2\text{O}_2$  by the exogenous

**Figure 6**

Dependence on pH of *S. asiatica* haustorial development induced by syringic acid or DMBQ. (a) With  $10^{-4}$  M syringic acid at pH 4.6 for two days. (b) With  $10^{-4}$  M syringic acid at pH 5.2 for two days. (c) With  $10^{-5}$  DMBQ at pH 4.2 for two days. (d) With  $10^{-5}$  M DMBQ at pH 8.0 for two days. (e, f) With  $10^{-4}$  M syringic acid at pH 5.6 for two days. Scale bars: (a–e) 100  $\mu$ m; (f) 30  $\mu$ m.



application of catalase (an enzyme that breaks down  $H_2O_2$ ). Bovine liver catalase (EC 1.11.1.6) proved to be very efficient, rapidly removing  $H_2O_2$  from the *in vitro* assays and blocking peroxidase-catalyzed phenol conversion. In the presence of DMBQ,  $10^{-2}$  to  $>10^3$  units of catalase per ml, had no effect on haustorial induction. At  $10^{3.2}$  units per ml, however, catalase completely inhibited haustorial induction by  $10^{-4}$  M syringic acid, indicating a requirement for peroxidase in generating the signaling molecule from syringic acid. The magnitude of the inhibition gradually diminished with lower catalase concentrations, such that below  $10^{-2}$  units per ml, normal haustorial induction ensued.

#### Cloning of *Striga* peroxidase cDNAs

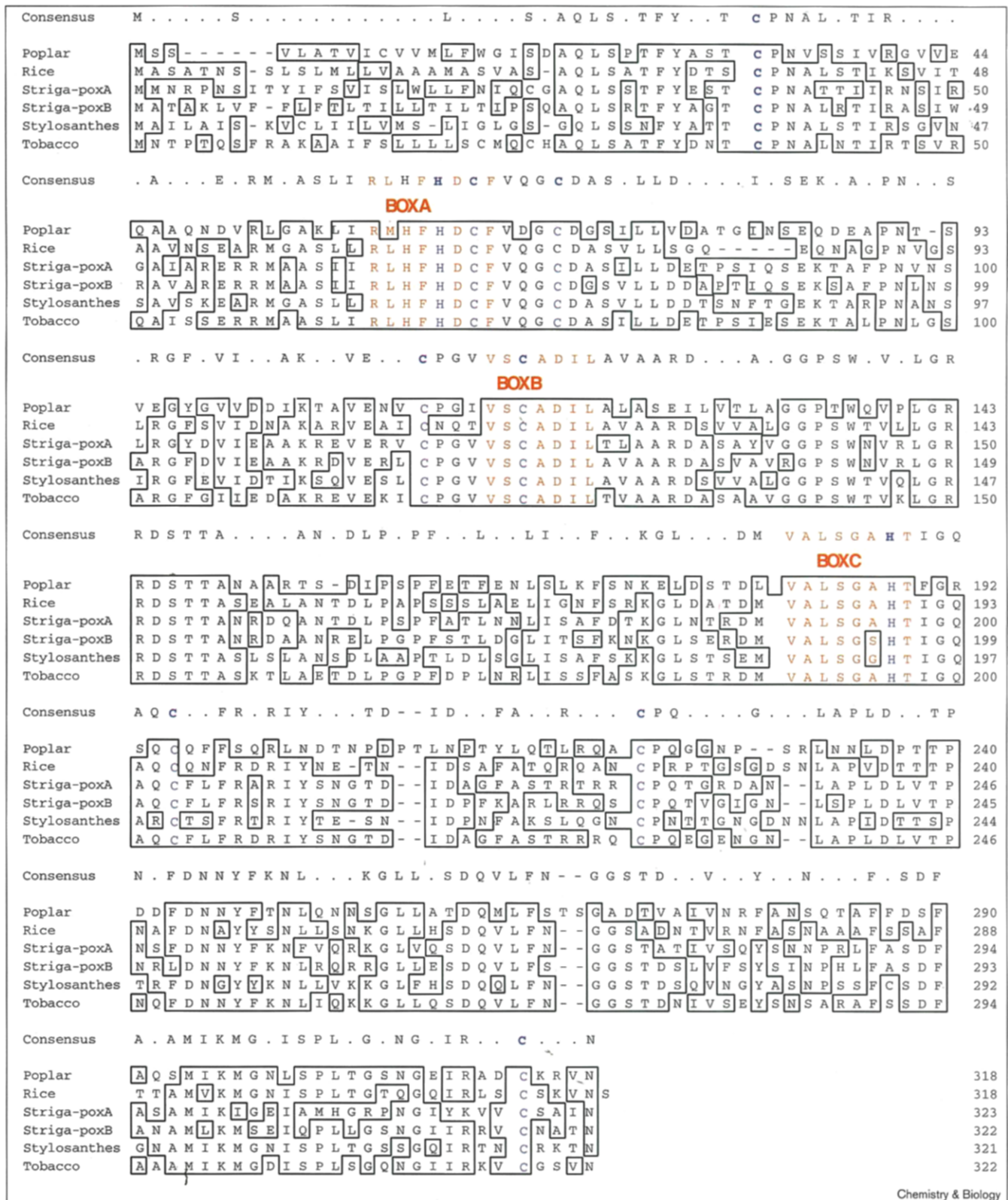
Although the accumulated evidence established that the extracted peroxidases were essential for the oxidation of phenols to quinone inducers, a role for these enzymes in host recognition had not yet been established. Genes encoding peroxidases from several plants have been sequenced [30,31] and two amino-acid stretches from conserved regions, around the catalytic domain (box A; Figure 7) and the heme-binding domain (box C; Figure 7), were used to design degenerate oligonucleotide primers. The first primer (P-I) was based on the peptide sequence RLHFHDCF (using single-letter amino-acid code) of box A, and the second primer (P-II) was based on the sequence VALSGAHT of box C. Polymerase chain reaction (PCR)

amplification using these degenerate primers with cDNA prepared from total RNA of 2 day-old *S. asiatica* seedlings yielded a band of the expected size, approximately 420 base pairs. Several independent candidate clones were sequenced from these and other degenerate primers and only two contained the conserved box B sequence. The deduced amino-acid sequences of the two different fragments strongly resembled each other, as well as those of other plant peroxidases. Repeated sequencing runs were used to confirm the base pair assignment. In order to isolate full-length cDNAs, gene-specific primers (PA-1, -2, -3, -4, PB-1, -2, -3, -4) were designed (Figure 8 shows their sequence origins). Following successful amplification, the products of 5'- and 3'- random amplification of cDNA ends (RACE) were gel-purified, subcloned and sequenced. These procedures enabled us to isolate the full-length *S. asiatica* cDNAs designated *poxA* and *poxB*.

#### Characterization of the *Striga* peroxidase genes

The eight conserved cysteines and two invariant histidines of the plant peroxidases [30,31] are encoded in the *poxA* and *poxB* genes (Figure 8). Histidine 68/69 has been predicted to be involved in acid/base catalysis and belongs to the highly conserved subdomain box A. Histidine 195/196 in the highly conserved subdomain box C is predicted to serve as the fifth ligand to the heme iron. Between these two conserved subdomains, there is another conserved region of seven amino acids, VSCADIL, designated box B. Putative

Figure 7



Multiple alignment of the amino-acid sequences of the plant peroxidases and the derived *Striga* peroxidase A (PoxA) and peroxidase B (PoxB) sequences. The highly conserved regions are marked Box A, Box B and Box C.

sites of *N*-glycosylation (asparagine-X-threonine/serine, where X is any amino acid) were found at amino-acid positions 40 and 213 of PoxA and at positions 180, 212, 236, and 318 of PoxB (Figure 8). The diffuse nature of the bands seen in the isoelectric focusing experiments in Figure 3 might be due to differential glycosylation of the peroxidase proteins.

The full-length cDNAs isolated using RACE had 110 base pairs of 5'- and 150 base pairs of 3'-untranslated sequences, each including the possible polyadenylation signal AATAAA. This sequence is located 28 nucleotides before the poly(A) stretch in *poxA* (Figure 8). The deduced amino-acid sequences each contain an amino-terminal signal sequence with a hydrophobic core and the predicted cleavage site at an alanine [32] (Figure 8). The length of the signal sequences are 27 and 26 amino acids, respectively, for *poxA* and *poxB*. The mature proteins for peroxidase A and peroxidase B each contain 295 amino acids with predicted molecular weights of 35,250 Da and 35,252 Da and calculated pI's of 8.6 and 9.3, respectively. Although there is a very broad range of homology throughout the known plant peroxidases, from 30% to 70%, the two cDNAs share 67% identity with each other in their coding sequence and their predicted amino acid sequences are 67.1% homologous. Several closely related genes are known and are compared in the dendrogram in Figure 9.

#### **Expression of *poxA* and *poxB* during *Striga* development**

The relative expression levels of the *Striga* peroxidase genes during development were determined using quantitative PCR. In order to quantify the amounts of *poxA* and *poxB* mRNAs, gene-specific primers (PA-1, PA-3, PB-1, PB-3) were used to amplify different-sized products, a 316 base-pair product from *poxA* (using PA1/PA3) and a 333 base-pair product from *poxB* (using PB-1/PB-3). The recombinant plasmid DNAs were used to prepare standard curves for quantitative PCR with the 5' end-labeled primer. The amount of the first-strand cDNAs primed by oligo(dT) from total RNA of different stage *S. asiatica* seedlings was adjusted to fall within the linear range of the PCR experiments. Neither *poxA* nor *poxB* mRNA was detectable in the mature plant tissues or in preconditioned seeds prior to addition of the germination stimulant (Figure 10). Following addition of the SXSg germination stimulant, expression of both peroxidases increased within the first 24 h, roughly the time required for emergence of the seedling from the seed coat, and remained constant for several days. This expression, however, was reduced within hours of exposure of the seedling to DMBQ. Clearly, the expression of *poxA* and *poxB* is therefore regulated during early seedling growth and during haustorial induction in *S. asiatica* and appears not to occur in the aerial parts of the plant. This pattern of regulation was consistent with the histochemical staining data.

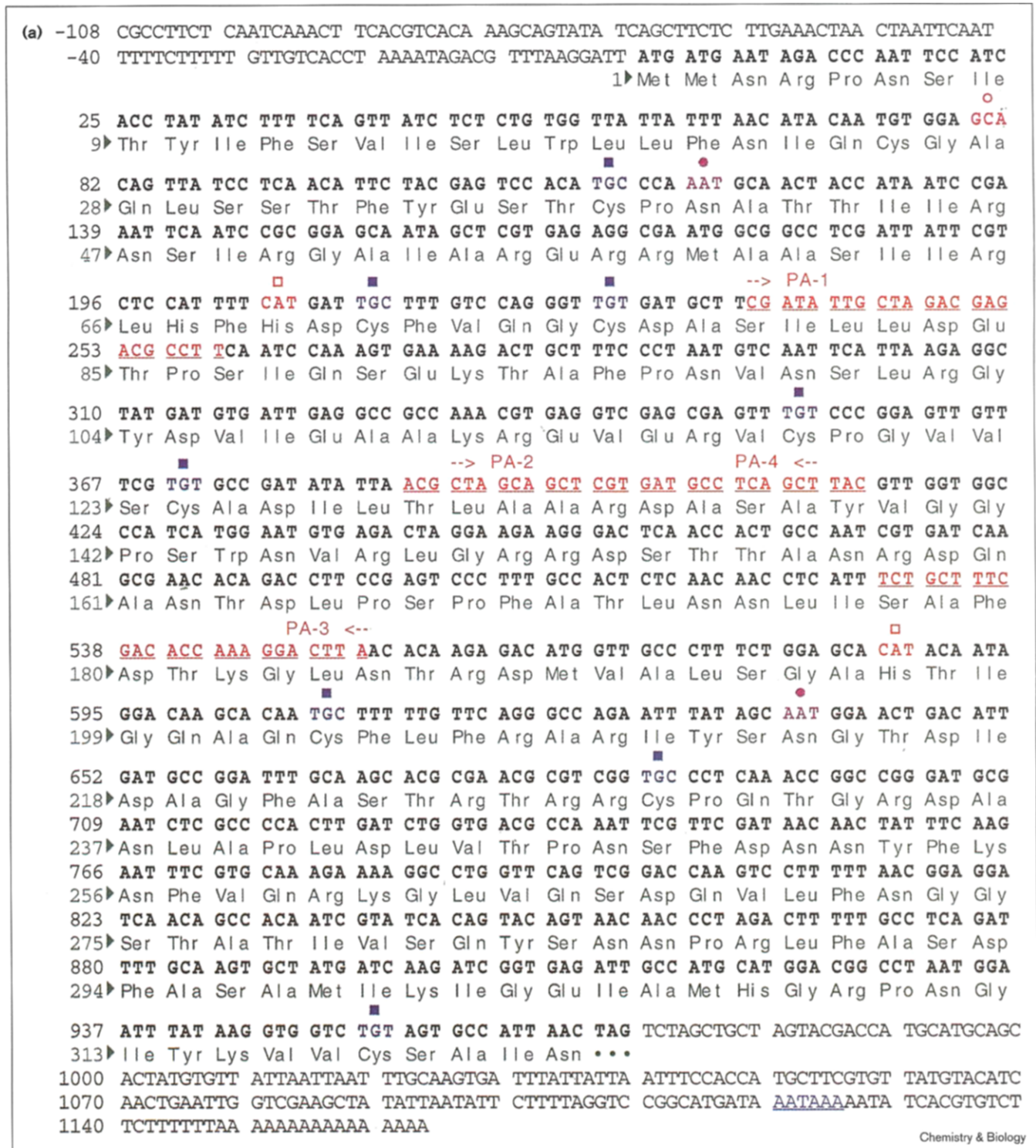
## **Discussion**

*Striga* spp. represent the major biotic constraint to grain production in sub-Saharan Africa and, as a result, have been studied extensively. Accordingly, *Striga* spp. are the best characterized parasitic plants with respect to the chemistry of host recognition and therefore are the most readily analyzed mechanistically. Parasitic phenol oxidases were implicated in host recognition as a result of two principal findings: washing *S. asiatica* seedlings rendered them unable to develop haustoria in response to their hosts, and, this loss of function was reconstituted by laccase. In this study, we show that the apoplastic oxidases removed by washing are peroxidases with broad substrate specificity, capable of oxidizing known haustorial-inducing phenols to benzoquinones, and that these enzymes are dependent on pH in a pattern that correlates precisely with the pH dependence required for phenol induction of haustoria. Moreover, removal of the peroxidase co-substrate, H<sub>2</sub>O<sub>2</sub>, abolishes phenol induction of haustoria. Because quinone haustorial induction is independent of both pH and H<sub>2</sub>O<sub>2</sub>, the cloned peroxidases must function upstream of quinone detection in the conversion of wide array of phenol inducers into a small subset of quinone signals.

A more important question is whether these apoplastic oxidases function to mediate host detection. In *S. asiatica*, the major commitment to the host is at the level of germination, but the transition from vegetative to parasitic growth is no less critical. Haustorial development in *S. asiatica* occurs at the root meristem and successful attachment of the parasite to the host requires that haustorial development is initiated only after host-parasite contact [12,19,29]. Histochemical studies clearly showed that the oxidase activity is localized uniquely to the meristem where such contact must occur. Localization of the oxidases in this fashion could appropriately restrict the host detection chemistry to the host-parasite interface, but issues regarding the control of oxidase expression, the nature of the reactions being catalyzed, and the uniqueness of the oxidases to the parasite must be resolved in order to address the issue of host recognition fully.

We found that *poxA* and *poxB* were the only oxidase genes expressed in young *Striga* seedlings. Both peroxidase genes contain leader sequences that are consistent with their apoplastic localization, and their predicted pI's are identical to those of the peroxidases found in the *S. asiatica* apoplast. The expression of *poxA* and *poxB* is activated by exposure to the germination signal, SXSg, and is suppressed by DMBQ. The speed and level of *Striga* peroxidase induction and repression represents a dramatic example of peroxidase regulation. There are now several examples of plant peroxidase gene regulation which ensure highly specific spatial and temporal localization of peroxidases. The peroxidases from barley [33], wheat [34] and rice [35] are induced by fungal pathogens; a cationic peroxidase from

Figure 8a



Nucleotide sequences, and deduced amino acid sequences, of *S. asiatica* peroxidase cDNAs. (a) PoxA and (b) PoxB. The gene-specific primers (PA-1,-2,-3,-4, PB-1,-2,-3, and -4) for RACE were designed from the cDNA sequences underlined. Solid lines designate the sense strand and the broken arrows the nonsense strand. The plant peroxidase conserved cysteines are marked with a filled blue box

and histidines with an open red box. Putative asparagine residues for *N*-glycosylation are marked with the filled purple circle, and the predicted cleavage site at alanine of the amino-terminal signal sequences are marked with the open red circle. The likely polyadenylation site AATAAA is underlined.



Figure 8b

```

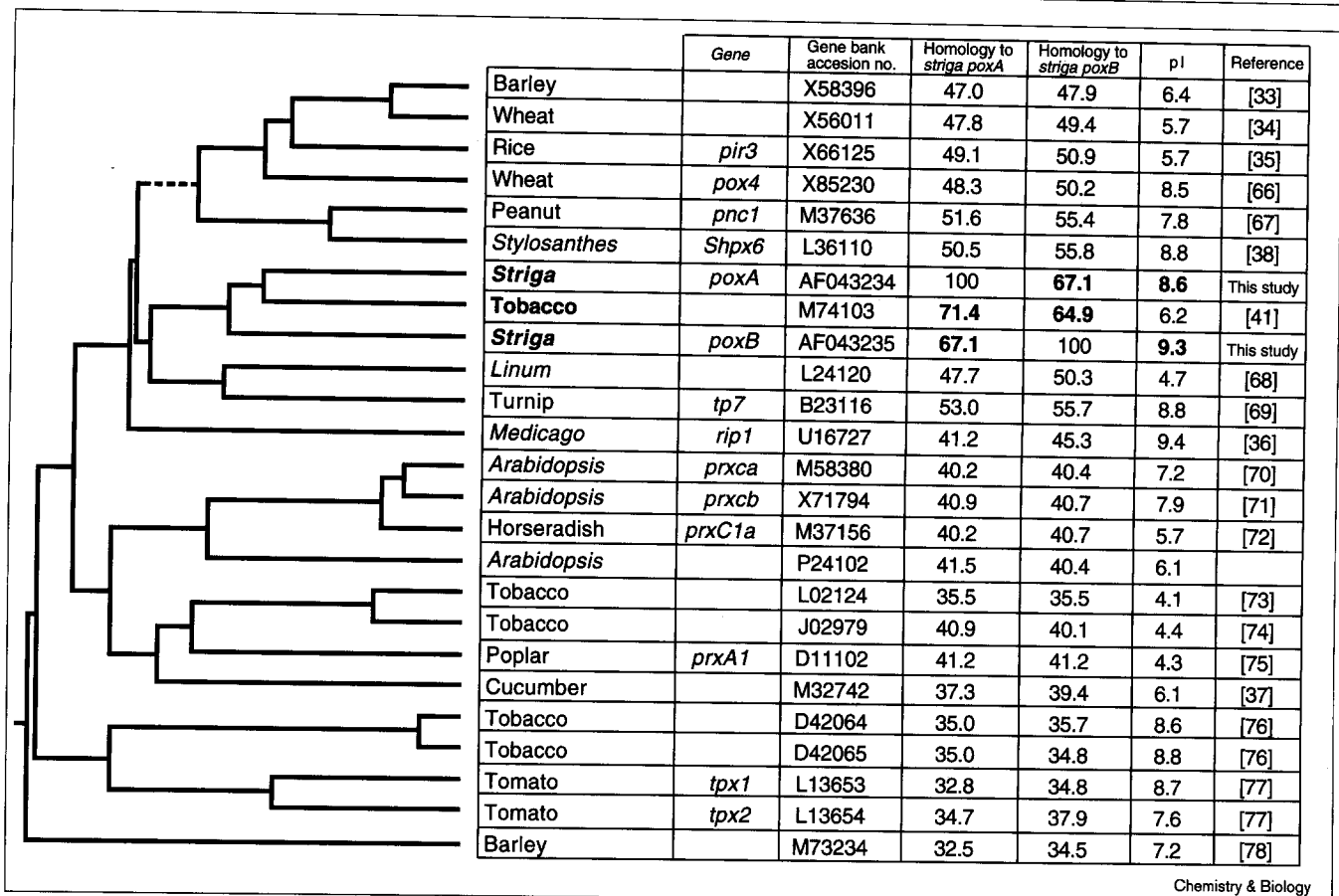
(b) -117 TCAACTT CACGTAAAAC GAAATTGCGT TGACTCGTTA CATTGTTCTGA TCCTTATACA TTGCCAGGAA
-50 AAAGGAAACG AAATATATAA TTCGAATTTG TCACCGTACT TTGTCTTAAC ATG GCC ACC GCA AAG
16 CTC GTC TTC TTT TTA TTC ACG CTA ACC ATA CTA CTC ACA ATA CTC ACA ATC CCA TCC
6▶ Leu Val Phe Phe Leu Phe Thr Leu Thr Ile Leu Leu Thr Ile Leu Thr Ile Pro Ser
73 CAA GCC CAG CTG TCC CGA ACT TTC TAT GCC GGT ACA TGT CCC AAT GCG CTG CGT ACA
25▶ Gln Ala Gln Leu Ser Arg Thr Phe Tyr Ala Gly Thr Cys Pro Asn Ala Leu Arg Thr
130 ATC CGT GCC TCG ATC TGG CGG GCT GTG GCG CGC GAG CGC CGC ATG GCA GCC TCG ATT
44▶ Ile Arg Ala Ser Ile Trp Arg Ala Val Ala Arg Glu Arg Arg Met Ala Ala Ser Ile
187 ATT CGT CTC CAT TTT CAT GAT TGC TTC GTG CAG GGC TGT GAT GGT TCG GTG TTG CTC
63▶ Ile Arg Leu His Phe His Asp Cys Phe Val Gln Gly Cys Asp Gly Ser Val Leu Leu
244 GAT GAT GCG CCC ACG ATC CAG AGT GAG AAG TCG GCT TTC CCT AAC TTG AAC TCC GCA
82▶ Asp Asp Ala Pro Thr Ile Gln Ser Glu Lys Ser Ala Phe Pro Asn Leu Asn Ser Ala
301 AGA GGG TTT GAC GTG ATT GAG GCC GCC AAG AGA GAT GTC GAG CGT TTG TGC CCA GGT
101▶ Arg Gly Phe Asp Val Ile Glu Ala Ala Lys Arg Asp Val Glu Arg Leu Cys Pro Gly
358 GTC GTC TCC TGT GCG GAC ATT CTG GCC GTG GCC GCA CGT GAT GCC TCG GTG GCG GTC
120▶ Val Val Ser Cys Ala Asp Ile Leu Ala Val Ala Ala Arg Asp Ala Ser Val Ala Val
415 CGT GGG CCG TCA TGG AAC GTG AGG CTC GGG AGA AGG GAC TCT ACC ACA GCT AAT CGT
139▶ Arg Gly Pro Ser Trp Asn Val Arg Leu Gly Arg Arg Asp Ser Thr Thr Ala Asn Arg
472 GAT GCG GCA AAC CGT GAA CTA CCG GGG CCA TTT TCC ACC CTT GAT GGC CTA ATC ACG
158▶ Asp Ala Ala Asn Arg Glu Leu Pro Gly Pro Phe Ser Thr Leu Asp Gly Leu Ile Thr
529 TCT TTT AAG AAT AAG GGC CTC AGT GAA AGA GAC ATG GTT GCC CTC TCT GGA TCA CAC
177▶ Ser Phe Lys Asn Lys Gly Leu Ser Glu Arg Asp Met Val Ala Leu Ser Gly Ser His
586 ACG ATC GGG CAA GCG CAG TGC TTC CTG TTC CGA AGC AGG ATC TAC AGC AAT GGC ACG
196▶ Thr Ile Gly Gln Ala Gln Cys Phe Leu Phe Arg Ser Arg Ile Tyr Ser Asn Gly Thr
643 GAT ATC GAT CCA TTC AAA GCC CGT CTG AGG AGA CAG TCT TGC CCT CAG ACG GTG GGG
215▶ Asp Ile Asp Pro Phe Lys Ala Arg Leu Arg Arg Gln Ser Cys Pro Gln Thr Val Gly
700 ATA GGC AAC CTT TCC CCA CTC GAC CTT GTA ACC CCC AAC AGG CTC GAC AAC AAC TAC
234▶ Ile Gly Asn Leu Ser Pro Leu Asp Leu Val Thr Pro Asn Arg Leu Asp Asn Asn Tyr
757 TTT AAG AAC CTT CGT CAA AGG AGG GGT CTC CTT GAG TCG GAC CAA GTC CTT TTT AGC
253▶ Phe Lys Asn Leu Arg Gln Arg Arg Gly Leu Leu Glu Ser Asp Gln Val Leu Phe Ser
814 GGG GGC TCT ACA GAC AGT CTA GTT TTC AGC TAC AGC ATA AAT CCT CAC CTA TTC GCC
272▶ Gly Gly Ser Thr Asp Ser Leu Val Phe Ser Tyr Ser Ile Asn Pro His Leu Phe Ala
871 TCC GAT TTC GCT AAT GCC ATG CTC AAG ATG TCT GAG ATT CAG CCA TTG CTC GGG TCG
291▶ Ser Asp Phe Ala Asn Ala Met Leu Lys Met Ser Glu Ile Gln Pro Leu Leu Gly Ser
928 AAT GGG ATC ATA AGG AGG GTT TGT AAC GCC ACA AAC TAA GTGCGCTGTT AAGAAATATT
310▶ Asn Gly Ile Ile Arg Arg Val Cys Asn Ala Thr Asn ...
987 GTTTGCGAAC ACTTCAAGAA AAGAAATAAC TAAAAGATAT ACTAGTGTITT GCGAATACTC
1047 TGTAATTGCG GCTGCGAGCG TATATATGGT GCTTGTATTG ATTTATAAAG CATATGGAAT
1107 TATGAATATG CTATTCTATA ATCTGGGCAT ATATGCAGAG AGATTATTTT ACGTAAAAAA AAAAA
    
```

Chemistry & Biology

*Medicago truncatula* is induced by its symbiotic *Rhizobium* spp. [36]; and an anionic cucumber peroxidase is induced by ethylene [37]. A cationic peroxidase of the tropical

forage legume *Stylosanthes humilis*, which is highly homologous to *poxA* and *poxB* (Figure 9), is strongly induced by the fungal phytopathogen *Colletotrichum gloeosporioides*

Figure 9



Chemistry &amp; Biology

Dendrogram showing the relationships among the deduced amino-acid sequences of the PoxA and PoxB proteins from *S. asiatica* and those of 23 other plant peroxidases. Percentage identity to the *Striga* PoxA

and PoxB are shown, and the pI is calculated from the deduced amino-acid sequence of each mature protein.

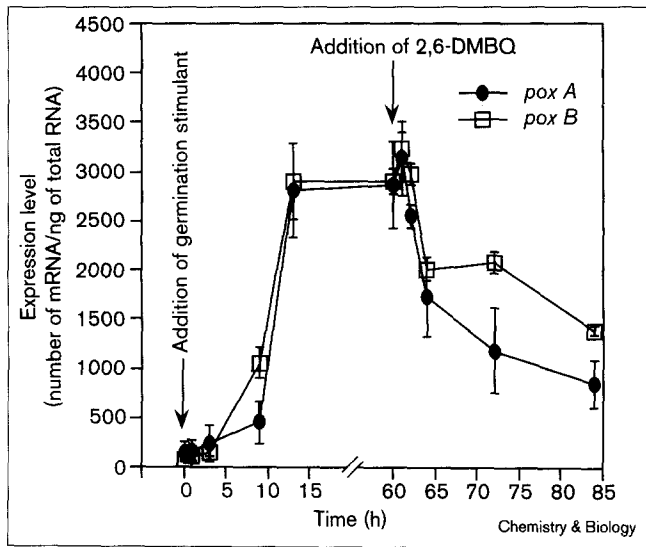
within 4 h of inoculation [38]. The peroxidase from *Nicotiana sylvestris* that is most similar to *Striga poxA* and *poxB* is highly expressed at the beginning of *Nicotiana sylvestris* protoplast regeneration and moderately in roots [39]. It appears therefore that the regulation of peroxidases at the transcriptional level is common and certainly important for their function.

The regulation of *poxA* and *poxB* may explain the formation of the multiple haustoria under certain conditions (shown in Figure 6e,f). DMBQ has been shown to be cleared *in vivo* [12] and, once cleared, new root primordia develop from the committed haustorium [29]. This new meristematic growth would activate expression of *poxA* and *poxB*, and, in the presence of excess phenol, the accumulating enzymes could catalyze DMBQ generation, which would start haustorial development over again. The formation of multiple haustoria, (Figures 6e,f), could be controlled through such a cyclic process; in the presence of excess syringic acid, oscillating peroxidase expression would result in sequential haustorial inductions. The

oscillation in expression of *poxA* and *poxB* could provide a mechanism for controlling the development of multiple haustoria *in vitro* [40,41].

The *Striga* PoxA and PoxB proteins are plant peroxidases that contain a ferriprotein porphyrin prosthetic group, four conserved disulfide bridges, an invariant aspartic acid-arginine salt bridge, and two calcium ions. Across the three different peroxidase classes, bacterial, mitochondrial, and chloroplast (Class 1), fungal (Class 2), and plant (Class 3), there is less than 20% sequence identity, but the catalytic residues in the heme cavity are highly conserved [31] and the reaction mechanism is shared. The broad redox range of peroxidases has been attributed to the relative position of the porphyrin within the protein [42], but it is likely that the broad product distribution is much more a function of the reaction pathways open to the phenoxy-radical intermediate generated by the one-electron oxidation chemistry of the reaction [25,26,43-45]. Certainly the pectic fractions from host cell walls contain phenolic substituents that are substrates for enzymes like PoxA and

Figure 10



The expression levels of *poxA* and *poxB* as determined using quantitative PCR during seedling development.

PoxB, and the products include quinones. Just as we have shown here for the model phenol, syringic acid, the host pectic wall fractions are oxidized to DMBQ [12].

PoxA and PoxB are, however, not unique to the *Striga* parasite, but are members of a large gene family. A survey of the literature suggests that the plant peroxidase genes are numerous, as many as 40 per plant [46]. This number of peroxidases would allow Fenton chemistry to be targeted to virtually every cellular compartment where a specific role of maintaining or adapting structures and functions of the plant cell to its environment must be met. In both *Arabidopsis*, which has a seed and radicle of similar size to *Striga*, and grass hosts, including maize and sorghum, the root hair zone has intense peroxidase activity. In the panicle grasses, both epidermal cells in the later regions of root elongation and root cap cells have apoplastic peroxidases in significantly higher abundance [27] than we found in *S. asiatica*. These host enzymes, which are homologous to PoxA and PoxB, are capable of the same generic Fenton chemistry, are abundant in the host walls where parasite attachment occurs, and are therefore quite capable of converting wall-localized phenols into quinones.

If PoxA and PoxB are not unique to the parasite and not involved in host recognition, how did the washing experiments, which removed these enzymes, remove host detection activity? Addition of horseradish peroxidase did not reconstitute the oxidase activity [12], but we have now found that the addition of  $H_2O_2$  to maize and sorghum seedlings does release significant haustorial-inducing activity (R.K., W.J.K and D.G.L., unpublished observations). Differentiation between host and parasite therefore lies in

the availability of the oxidant, not the oxidase. This conclusion is supported by the observation that chromophoric substrate coloration (confirmation of oxidase activity) develops slowly without added  $H_2O_2$  in *S. asiatica*, but not at all in the other plants tested.

The required oxidant,  $H_2O_2$ , is common in plants and has been assigned a variety of biological roles that range from a general antimicrobial agent to a specific signal molecule in systemic acquired resistance [47–49]. There is even evidence that it accumulates in the plant cell wall during pathogen invasion [50]. Several enzymes have been implicated in  $H_2O_2$  production, including apoplastic peroxidases [51,52], lipoxygenases and oxalate oxidase [53], each of which requires a reducing substrate to be supplied to the apoplast [54–57]. Alternatively, redox activity across the plasma membrane [58] could produce an active oxygen species directly. Oxidase complexes homologous to the human neutrophil oxidative burst machinery have been detected in plants [59–62]. Although the specific function of these oxidase complexes is unclear [63], the possibility of such a system is particularly interesting as xenogostic quinones were recently shown to be detected through a benzoquinone-dependent oxidoreductase whose terminal acceptor, based on the discovered redox range, is likely to be  $O_2$  [22]. An autocatalytic cycle connecting  $H_2O_2$  generation with quinone detection could greatly enhance the sensitivity of host detection and suggests that a single transmembrane oxidase would be sufficient for both activities.

Given the model that the oxidant is the limiting factor, there must be another difference between host and parasite, that is, the phenolic substrates must be available in the host wall, and absent from the parasite. In the grass hosts of *Striga*, the phenolic content in the primary walls of nonvascular tissues varies greatly, from 1/50 to 1/2,400 phenols per sugar residue, depending on the tissue type [27]. The finding that  $H_2O_2$  added to sorghum and maize roots released significant haustorial-inducing activity suggests that host phenols are accessible to the host peroxidases; these oxidation products must be further characterized to better understand the result, however. Addition of  $H_2O_2$  to *Striga* roots does not induce haustoria, suggesting that either the phenolic substrates are not present in the parasite wall or they are not available to PoxA/PoxB.

In *Agalinis purpurea*, a related hemi-parasitic Scrophulariaceae in which meristem-localized oxidase activity has also been detected [19], haustoria are induced by phenols in agar plate cultures [64]. In two week-old cultures, however, spontaneous haustoria begin to develop and self-attachment is common in these as well as in other Scrophulariaceae [20]. In *S. asiatica*, the roots never mature more than 5 days past germination because of limited food reserves in the seed [12]. Initial extraction

experiments have shown that these young seedlings have reduced phenolic content, and the isolated walls are devoid of haustorial-induction activity. The parasitic plants may therefore capitalize on the low phenolic epithelial wall content of the juvenile roots in order to exploit the critical difference between the hosts and the parasites, namely the constitutive production of  $H_2O_2$ .

### Significance

The loss of autonomy and the acquisition of traits that enforce the dependence of one organism on another is a central feature of the evolution of genome structure. In the parasitic plants, elements of genome autonomy are lost and it appears possible to understand the molecular events that have driven this evolution by characterizing the events that initiate attachment organ development. From a practical point of view, parasitic plants represent a serious constraint on agricultural productivity and insight into the mechanism of initiating parasite development in one organism might open general strategies for control.

*Striga asiatica* respond to a diverse array of known molecular structures in order to induce the parasitic mode. The two peroxidases that we have identified in *Striga* root cell walls can account for the diversity of the inducing signals. Identification of these peroxidases does not, however, provide support for the hypothesis that a parasitically exuded oxidase mediates host detection. We propose instead a new model which holds that the critical evolved difference between host and parasite is the constitutive production of an activated oxygen species, via reduction of  $O_2$ . Furthermore, both host and parasite play an active role in host detection. Detection of host root surfaces exploits both host-wall phenolic content, which may be a function of organ maturity, and host enzymes. The parasite is therefore asking two questions—Do the walls contain the phenol substrate? And are there enzymes available to convert the substrates to the quinone signal?—which increase the precision of its commitment to the parasitic mode. Finally, the model is consistent with the idea that  $H_2O_2$  production is coupled with detection of the haustorial induction signal in an autocatalytic cycle to enhance host detection sensitivity.

### Materials and methods

#### Plant materials

*Striga* seeds were sterilized as previously described [22] and pretreated in  $H_2O$  at 27°C in the dark for 10 days. Pretreated seeds (100 mg) were used for germination and were collected after incubation (0 h, 1 h, 3 h, 9 h, and 13 h) with the SXSg germination stimulant [13,14]. Two-day-old germinated seedlings were exposed to  $2 \times 10^{-6}$  M of DMBQ and were collected after a series of incubations (0 h, 1 h, 2 h, 4 h, 12 h, or 24 h).

Sorghum Sudan Grass Hybrid seeds (20 g) were grown aseptically as described previously [13] and after 12 days the roots (4 g) were

removed, frozen in liquid nitrogen and lyophilized. The resulting brown powder was resuspended using sonication and washed  $4 \times @ 1,800$  g with 30 ml Tris-maleate buffer, pH 7.8, containing 1% Triton X100, washed with EtOH, and lyophilized to a gray powder (0.5 g). Extraction in boiling  $H_2O$  overnight solubilized the pectic fraction. Saponification in 0.2 M KOH under  $N_2$ , neutralization with dilute HCl, and  $Et_2O$  extraction gave the organic soluble fraction [28,65].

#### Histochemical staining

*Striga* seedlings were taken from the germination media and transferred to the peroxidase assay solution containing 10 mM sodium phosphate, 0.03%  $H_2O_2$ , and 0.2% pyrogallol. Oxidation of pyrogallol results in reddish coloration of the tissue that is visible within 2–5 min. Following color development, seedlings were rinsed with dd $H_2O$ . Oxidation of syringaldazine results in a red–purple color. When the seedlings were stained with syringaldazine they were transferred to microscope slides and a solution of the dye in 0.1% in EtOH (1–2 drops), followed by 0.3%  $H_2O_2$  (1–2 drops) was added. The red–purple color tended to fade after 15 min.

#### RNA isolation and first strand cDNA synthesis

Total RNAs were isolated from 2 day-old *Striga* seedlings (100 mg) by phenol/chloroform extraction (Promega Total RNA isolation kit). The yield of total RNA obtained was determined spectrophotometrically at 260 nm, where one A260 unit = 40  $\mu$ g of single stranded RNA/ml. First strand cDNAs were synthesized from 2  $\mu$ g of total RNA with 0.5  $\mu$ g of oligo(dT)12–18 using SuperScript II RNase H–Reverse Transcriptase (Life Technologies). The RNA was digested with *E. coli* RNase H and the resulting single stranded cDNA was used for PCR amplification.

#### PCR amplification of the peroxidase genes

PCR reactions were carried out in 100  $\mu$ l of buffer containing the first strand cDNA from 2  $\mu$ g of total RNAs, 75 pmol each of the degenerate primers (P–I, P–II), 5 units of AmpliTaq DNA polymerase (Perkin-Elmer), 20 mM Tris–HCl (pH 8.4), 50 mM KCl, 2.5 mM  $MgCl_2$ , 0.1  $\mu$ g BSA, 0.5 mM dATP, 0.5 mM dGTP, 0.5 mM dCTP, 0.5 mM dTTP, and 10 mM dithiothreitol (DTT). Following an initial 5 min denaturation at 95°C, 35 cycles of PCR amplification were performed with 1 min denaturation at 94°C, 1 min annealing at 45°C, and 2 min extension at 72°C that was increased by 6s in each subsequent cycle.

#### Subcloning and DNA sequencing

The amplified PCR products were analyzed by gel electrophoresis in 4% Nusieve agarose. PCR products were purified from the agarose gel and subcloned using the pCR-Script™ SK(+) Cloning kit (Stratagene) according to the manufacturer's instructions. Putative recombinant plasmids carrying inserts of the appropriate size were used for DNA sequencing. All DNA sequencing was performed on double-stranded plasmid templates by the dideoxy chain termination method with Sequenase version 2.0 kit (United States Biochemical Co.).

#### Cloning of full-length peroxidase cDNAs

5′-RACE and 3′-RACE experiments utilized the materials from Life Technologies. The gene-specific primers were designed from the cDNA sequences of cloned genes. PCR reactions were conducted with AmpTaq polymerase (Perkin Elmer) according to the manufacturer's conditions. For 3′-RACE, first strand cDNAs were synthesized from total RNA using the chimeric adaptor primer (AP), which contained both oligo(dT)17 and the amplification primer (UAP), and PCR-amplified using the gene specific primers, PA-1 or PB-1, and UAP. Second round PCR was carried out with a nested gene specific primer, PA-2 or PB-2, and UAP. For 5′-RACE, first strand cDNAs were synthesized from total RNA using gene specific primers PA-3 or PB-3. After RNase treatment, an anchor sequence, oligo dC, was added to the 3′ end of the cDNA using terminal transferase and dCTP. The cDNA products were PCR-amplified using nested gene specific primers PA-4 or PB-4 and a chimeric anchor primer ANP. Following amplification, the products of 5′- and 3′-RACE were gel-purified, subcloned, and sequenced as described above.

### Quantitative PCR

In order to quantify the amplified products, primers (10 pmol) were labeled with 50  $\mu\text{Ci}$  of [ $\gamma$ - $^{32}\text{P}$ ]-ATP (6,000 Ci/mmol, Amersham) by T4 polynucleotide kinase (Life Technologies, Inc). The optimized buffer condition for each primer set was determined using the PCR Optimization kit (Stratagene). With the optimized conditions, standard curves were constructed for each clone-primer combination using labeled primers (100  $\mu\text{Ci}$ /pmol of primer per 25  $\mu\text{l}$  reaction volume). Control reactions contained a mixture of two peroxidase clones ranging from 0.1 pg to 10 pg of plasmid. After the initial denaturation of the template DNA at 94°C for 5 min, 25 cycles of PCR amplification were performed with 0.5 min of denaturation at 94°C, 1 min of annealing at 45°C and 1 min of extension at 72°C. After PCR, the amplified products were resolved on a 4% Nusieve-agarose gel and the gel was dried at 55°C in vacuo for 2 h. The amplified products on the dried gel were visualized by the use of a Phosphor Imager system. Standard curves were determined by plotting the counts of the amplified band vs. the initial template DNA. First strand cDNAs primed by oligo (dT) were used to measure the expression level of *poxA* and *poxB* in *Striga* seedlings.

### Oligonucleotide synthesis

Two degenerate oligonucleotides, P-I 5'-CAGGTCGACCGI(T/C)TICA(C/T)TT(C/T)CA(C/T)GA(C/T)TG(C/T)TT-3' and P-II 5'-GCCGGATCC-TT(G/A)TGI GCICCI(G/C)(A/T)IA(G/A)IGCIAC-3' were synthesized as primers for PCR amplification of peroxidase genes. The gene specific primers, PA-1 5'-CGATATTGCTAGACGAGACGCCTT-3', PA-2 5'-CT-AGCAGCTCGTGATGCCTCAGCTTAC-3', PA-3 5'-TAAGTCCTTTG-TGTGCGAAAGCAGA-3', and PA-4 5'-AGCTGAGGCATCACGAGCT-GCTAGCGT-3' were designed from the sequences of the cloned cDNA of peroxidase-A. PB-1 5'-ATGGTTCGGTGTGCTCGATGATG-3', PB-2 5'-GTGGCCGCACGTGATGCCTCGGTGGCG-3', PB-3 5'-GTCTCT-TTCACTGAGGCTCTTATTC-3', and PB-4 5'-CACCGAGGCATCAC-GTGGCCGACGGC-3' were designed from the sequences of peroxidase-B cDNAs. The adaptor primer, AP 5'-GGCCACGCGTCTGACT-AGTAC(T)<sub>17</sub>-3', the amplification primer, UAP 5'-CUACUACUACU-AGGCCACGCGTCTGACTAGTAC-3' and the anchor primer, ANP 5'-CUACUACUACUAGGCCACGCGTCTGACTAGTACGGIIGGGIIG-GGIIG-3' for 5'- and 3'-RACE were purchased from Life Technologies.

### Fractionation of oxidases bound to the cell wall from *Striga* seedlings

Frozen *Striga* seedlings (100 mg wet weight) were ground in a pre-chilled mortar and pestle in 1 ml of Extraction Buffer (25 mM Tris-HCl pH 7.0, 2 mM EDTA, 2 mM  $\beta$ -mercaptoethanol). The slurry was centrifuged at 15,000 g for 10 min and the pellet was washed twice in 500  $\mu\text{l}$  of Extraction Buffer containing 1% Triton. The insoluble cell wall fraction was recovered by retention on a 0.22  $\mu\text{m}$  filter. Proteins were extracted from the cell wall fraction by incubation in 500  $\mu\text{l}$  of Extraction Buffer containing 1 M NaCl for 1.5 h on ice with gentle shaking. The extracted protein was recovered by passage through a 0.22  $\mu\text{m}$  filter. The filtrate was de-salted against Extraction Buffer and concentrated by amicon ultrafiltration. Protein concentration was determined by Coomassie protein assay (PIERCE) and the individual proteins were resolved by isoelectrofocusing (Novex precast gel; pl 3.0–10.0). After electrofocusing, the gel was incubated in 10 mM sodium phosphate buffer (pH 6.0) for 10 min and the peroxidase activity was determined by 10 min immersion in peroxidase assay solution (PIERCE). The reaction was stopped by rinsing with water.

### Peroxidase assays

Peroxidase activity in cell wall extracts was quantified by conversion of syringic acid to DMBQ. Cell wall extracts were incubated at 30°C for various times in 100  $\mu\text{l}$  of buffer containing 20  $\mu\text{M}$  syringic acid, 25  $\mu\text{M}$   $\text{H}_2\text{O}_2$  and 50 mM sodium phosphate (pH 6.0 to 8.0) or sodium acetate (pH 4.0 to 5.5) and a portion of the reaction mixture was applied directly to a high performance liquid chromatography (HPLC) column (Zorbax ODS 0.46 i.d.  $\times$  25 cm, AcOH/MeOH/ $\text{H}_2\text{O}$ , 3.0/24.7/75.0, 1.0 ml/min, detection at 284 nm). The conversion was determined by comparing integrated peak areas with standard curves constructed

from syringic acid and DMBQ standards. Background oxidation without the peroxidase or without  $\text{H}_2\text{O}_2$  was insignificant.

### Catalase assays

*Striga* seeds (15–30) were placed in each of the 24 wells of a microtiter plate and germinated with a  $10^{-9}\text{M}$  solution of strigol over a 12 h period. Following a wash with sterile deionized water, the seedlings were allowed to grow for another 12 h before the addition of bovine liver catalase (EC 1.11.1.6), from  $1.7 \times 10^3$  to  $1.7 \times 10^{-2}$  units per ml, and syringic acid ( $10^{-4}\text{M}$ ). The percentage of haustoria was determined after an additional 36 h of incubation. Each assay was performed in triplicate and expressed as  $\pm$  SD. One unit of catalase is defined as the amount of solid that will decompose 1.0  $\mu\text{mol}$  of  $\text{H}_2\text{O}_2$   $\text{min}^{-1}$  at pH 7.0 and 25°C, with an initial concentration of  $\text{H}_2\text{O}_2 \geq 10.0$  mM.

### Acknowledgements

We are indebted to Robert Eplee and Rebecca Norris at the USDA Laboratory in Oxford, NC for providing seeds of *Striga asiatica* and grateful to the US Department of Energy ER20024 and the Rockefeller Foundation for financial support.

### References

- Kuijt, J. (1969). *The Biology of Parasitic Flowering Plants*. University of California Press, Berkeley.
- Atsatt, P.R. (1983). Host-parasite interactions in higher plants. In *Encyclopedia of Plant Physiology*. (Lange, O.L., Nobel, P.S., Osmond, C.B. & Ziegler, H., eds.), pp. 519-535, Springer-Verlag, Berlin.
- Molau, U. (1995). Reproductive ecology and biology. In *Parasitic Plants*. (Press, M.C. & Graves, J.D., eds.), pp. 141-176, Chapman & Hall, London.
- Musselman, L.J. & Press, M.C. (1995). Introduction to parasitic plants. In *Parasitic Plants*. (Press, M.C. & Graves, J.D., eds.), pp. 1-13, Chapman & Hall, London.
- Searcy, D.G. (1970). Measurements by DNA hybridization *in vitro* of the genetic basis of parasitic reductions. *Evolution* **24**, 207-219.
- Searcy, D.G. & MacInnis, A.J. (1970). Measurements by DNA renaturation of the genetic basis of parasitic reductions. *Evolution* **24**, 796-806.
- dePamphilis, C.W. (1995). Genes and genomes. In *Parasitic Plants*, (Press, M.C. & Graves, J.D., eds.), pp. 177-205, Chapman & Hall, London.
- Cronquist, A. (1988). *The Evolution and Classification of Flowering Plants*. New York Botanical Garden, Bronx, NY.
- dePamphilis, C.W. & Palmer, J.D. (1990). Loss of photosynthetic and chlororespiratory genes from the plastid genome of a parasitic flowering plant. *Nature* **348**, 337-339.
- Wolfe, K.H., Morden, C.W. & Palmer, J.D. (1992). Function and evolution of a minimal plastid genome from a nonphotosynthetic parasitic plant. *Proc. Natl Acad. Sci. USA* **89**, 10648-52.
- Nickrent, D.L. & Starr, E.M.C. (1994). High rates of nucleotide substitution in a nuclear small subunit (18S) rDNA from holoparasitic flowering plants. *J. Mol. Evol.* **39**, 62-70.
- Lynn, D.G. & Chang, M. (1990). Phenolic signals in cohabitation: implications for plant development. *Annu. Rev. Plant Physiol. Plant Mol. Biol.* **41**, 497-526.
- Fate, G., Chang, M. & Lynn, D.G. (1990). Control of germination in *Striga asiatica*: chemistry of spatial definition. *Plant Physiol.* **93**, 201-207.
- Fate, G.W. & Lynn, D.G. (1996). Xenogonin methylation is critical in defining the chemical potential gradient that regulates the spatial distribution in *Striga* pathogenesis. *J. Am. Chem. Soc.* **118**, 11369-11376.
- Saunders, A.R. (1933). Studies in phanerogamic parasitism with particular reference to *Striga lutea* Lour. *Dept. Agric. S. Afr. Bull.* **128**, 1-57.
- Olivier, A., Benhamou, N. & Leroux, G.D. (1991). Cell surface interactions between sorghum roots and the parasitic weed *Striga hermonthica*: cytochemical aspects of cellulose distribution in resistant and susceptible host tissues. *Can. J. Bot.* **69**, 1679-90.
- Visser, J.H., Dörr, I. & Kollmann, R. (1990). Compatibility of *Alectra vogelii* with different leguminous host species. *J. Plant Physiol.* **135**, 737-745.

18. Riopel, J.L. & Timko, M.P. (1995). Haustorial initiation and differentiation. In *Parasitic Plants*, (Press, M.C. & Graves, J.D., eds.), pp. 39-79, Chapman & Hall, London.
19. Chang, M. & Lynn, D.G. (1986). The haustorium and the chemistry of host recognition in parasitic angiosperms. *J. Chem. Ecol.* **12**, 561-579.
20. Yoder, J.I. (1997). A species-specific recognition system directs haustorium development in the parasitic plant *Triphysaria* (Scrophulariaceae). *Planta* **202**, 407-413.
21. Siquiera, J.O., Nair, M.G., Hammerschmidt, R. & Safir, G.R. (1991). Significance of phenolic compounds in plant-soil-microbial systems. *Crit. Rev. Plant Sci.* **10**, 63-121.
22. Smith, C.E., Rutledge, T., Zeng, Z., O'Malley, R. & Lynn, D.G. (1996). Redox control of development: the haustorium of *Striga asiatica*. *Proc. Natl Acad. Sci. USA* **93**, 6986-6991.
23. Boone, L.S. (1993). Mechanisms controlling developmental transitions in *Striga asiatica*. Ph.D. thesis, The University of Chicago.
24. Rutledge, T.R. (1992). The involvement of a redox process in development. Ph.D. thesis, The University of Chicago.
25. Caldwell, E.S. & Steelick, C. (1969). Phenoxyl radical intermediates in the enzymatic degradation of lignin model compounds. *Biochim. Biophys. Acta.* **184**, 420-431.
26. Umezawa, T., Nakatsubo, F. & Higuchi, T. (1982). Lignin degradation by *Phanerochaete chrysosporium*: metabolism of a phenolic phenylcoumaran substrate model compound. *Arch. Microbiol.* **131**, 124-128.
27. Smith, M.M. & O'Brien, T.P. (1979). Distribution of autofluorescence and esterase and peroxidase activities in the epidermis of wheat roots. *Aust. J. Plant Physiol.* **6**, 201-219.
28. Kay, L.E. & Basile, D.V. (1987). Specific peroxidase isoenzymes are correlated with organogenesis. *Plant Physiol.* **84**, 99-105.
29. Smith, C.E., Dudley, M.W. & Lynn, D.G. (1990). Vegetative/parasitic transition: control and plasticity in *Striga* development. *Plant Physiol.* **93**, 208-215.
30. Tyson, H. (1991). Relationships, derived from optimum alignments, among amino acid sequences of plant peroxidases. *Can. J. Bot.* **70**, 543-556.
31. Welinder, K.G. (1992). Superfamily of plant, fungal, and bacterial peroxidases. *Curr. Opin. Struct. Biol.* **2**, 388-393.
32. von Heijne, G. (1983). Patterns of amino acids near signal-sequence cleavage sites. *Eur. J. Biochem.* **133**, 17-21.
33. Thordahl-Christensen, H., et al. & Collinge, D. (1992). cDNA cloning and characterization of two barley peroxidase transcripts induced differentially by the powdery mildew fungus *Erysiphe graminis*. *Physiol. Mol. Plant Pathol.* **40**, 395-409.
34. Rebmann, G.H.C., Bull, J., Mauch, F. & Dudler, R. (1991). Cloning and sequencing of cDNAs encoding a pathogen-induced putative peroxidase of wheat (*Triticum aestivum* L.). *Plant Mol. Biol.* **16**, 329-331.
35. Reimann, C., Ringli, C. & Dudler, R. (1992). Complementary DNA cloning and sequence analysis of a pathogen-induced peroxidase from rice. *Plant Physiol.* **100**, 1611-1612.
36. Cook, D., Dreyer, D., Bonnet, D., Howell, M., Nony, E. & VandenBosch, K. (1995). Transient induction of a peroxidase gene in *Medicago truncatula* precedes infection by *Rhizobium meliloti*. *Plant Cell* **7**, 43-55.
37. Morgens, P.H., Callahan, A.M., Dunn, L.J. & Abeles, F.B. (1990). Isolation and sequencing of cDNA clones encoding ethylene-induced putative peroxidases from cucumber cotyledons. *Plant Mol. Biol.* **14**, 715-725.
38. Harrison, S.J., Curtis, M.D., McIntyre, C.L., Maclean, D.J. & Manners, J.M. (1995). Differential expression of peroxidase isogenes during the early stages of infection of the tropical forage legume *Stylosanthes humilis* by *Colletotrichum gloeosporioides*. *Mol. Plant Microbe Interact.* **8**, 398-406.
39. Criqui, M.C., et al. & Fleck, J. (1992). Characterization of genes expressed in mesophyll protoplasts of *Nicotiana sylvestris* before the re-initiation of the DNA replicational activity. *Mech. Dev.* **38**, 121-132.
40. Visser, J. & Dörr, I. (1987). The haustorium. In *Parasitic Weeds in Agriculture*, Volume 1: *Striga*. (Musselman, L.J., ed.), pp. 92-106, CRC Press, Boca Raton.
41. Wolf, S.J. & Timko, M.P. (1991). *In vitro* root culture - a novel approach to study the obligate parasite *Striga asiatica* (L.) Kuntze. *Plant Sci.* **73**, 233-242.
42. Ortiz de Montellano, P.R. (1987). Control of the catalytic activity of prosthetic heme by the structure of heme proteins. *Accounts Chem. Res.* **20**, 289-94.
43. Kaplan, D.C. (1979). Reactivity of different oxidases with lignins and lignin model compounds. *Phytochemistry* **18**, 1917-1919.
44. Gierer, J. & Opara, A.E. (1973). Studies on the enzymatic degradation of lignin. The action of peroxidase and laccase on monomeric and dimeric model compounds. *Acta Chem. Scand.* **27**, 2909-2922.
45. Young, M. and Steelink, C. (1973). Peroxidase-catalyzed oxidation of naturally occurring phenols and hardwood lignins. *Phytochemistry* **12**, 2851-2861.
46. Kjærsgård, I.V.H., Jespersen, H.M., Rasmussen, S.K. & Welinder, K.G. (1997). Sequence and RT-PCR analysis of two peroxidases from *Arabidopsis thaliana* belonging to a novel evolutionary branch of plant peroxidases. *Plant Mol. Biol.* **33**, 699-708.
47. Baker, C.J. & Orlandi, E.W. (1995). Active oxygen in plant pathogenesis. *Ann. Rev. Phytopathol.* **33**, 299-321.
48. Staskawicz, B.J., Ausubel, F.M., Baker, B.J., Ellis, J.G. & Jones, J.D.G. (1995). Molecular genetics of plant disease resistance. *Science* **268**, 661-667.
49. Levine, A., Tenhaken, R., Dixon, R. & Lamb, C. (1994). H<sub>2</sub>O<sub>2</sub> from the oxidative burst orchestrates the plant hypersensitive disease resistance response. *Cell* **79**, 583-593.
50. Bestwick, C.S., Brown, I.R., Bennett, M.H.R. & Mansfield, J.W. (1997). Localization of hydrogen peroxide accumulation during the hypersensitive reaction of lettuce cells to *Pseudomonas syringae* pv phaseolicola. *Plant Cell* **9**, 209-221.
51. Vera-Estrella, R., Blumwald, E. & Higgins, V.J. (1992). Effect of specific elicitors of *Cladosporium fulvum* on tomato suspension cells. *Plant Physiol.* **99**, 1208-1215.
52. Bolwell, G.P., Butt, V.S., Davies, D.R. & Zimmerlin, A. (1995). The origin of the oxidative burst in plants. *Free Radic. Res.* **23**, 517-532.
53. Zhang, Z.G., Collinge, D.B. & Thordal-Christensen, H. (1995). Germin-like oxalate oxidase, a H<sub>2</sub>O<sub>2</sub>-producing enzyme, accumulates in barley attacked by the powdery mildew fungus. *Plant J.* **8**, 139-145.
54. Halliwell, B. (1978). Lignin synthesis: the generation of hydrogen peroxide and superoxide by horseradish peroxidase and its stimulation by manganese (II) and phenols. *Planta* **140**, 81-88.
55. Mader, M. & Amberg-Fisher, V. (1982). Role of peroxidase in the lignification of tobacco cells. I. Oxidation of nicotinamide adenine dinucleotide and formation of hydrogen peroxide by cell wall peroxidases. *Plant Physiol.* **70**, 1128-1131.
56. Vianello, A. & Macri, F. (1991). Generation of superoxide anion and hydrogen peroxide at the surface of plant cells. *J. Bioenerg. Biomembr.* **23**, 409-423.
57. Pichorner, H., Couperus, A., Korori, S.A.A. & Ebermann, R. (1992). Plant peroxidase has thiol oxidase activity. *Phytochemistry* **31**, 3371-3374.
58. Rubinstein, B. and Luster, D.G. (1993). Plasma membrane redox activity: components and role in plant processes. *Annu. Rev. Plant Physiol. Plant Mol. Biol.* **44**, 131-55.
59. Auh, C.-K. & Murphy, T.M. (1995). Plasma membrane redox enzyme is involved in the synthesis of O<sub>2</sub><sup>-</sup> and H<sub>2</sub>O<sub>2</sub> by *Phytophthora* elicitor-stimulated rose cells. *Plant Physiol.* **107**, 1241-1247.
60. Tenhaken, R., Levine, A., Brisson, L.F., Dixon, R.A. & Lamb, C. (1995). Function of the oxidative burst in hypersensitive disease resistance. *Proc. Natl Acad. Sci. USA* **92**, 4158-4163.
61. Dwyer, S.C., Legendre, L., Low, P.S. & Leto, T.L. (1996). Plant and human neutrophil oxidative burst complexes contain immunologically related proteins. *Biochim. Biophys. Acta* **1289**, 231-237.
62. Groom, Q.J., Torres, M.A., Fordham-Skelton, A.P., Hammond-Kosack, K.E., Robinson, N.J. & Jones, J.D.G. (1996). *rbohA*, a rice homologue of the mammalian *gp91phox* respiratory burst oxidase gene. *Plant J.* **10**, 515-522.
63. Trost, P., Foscarini, S., Preger, V., Bonora, P., Vitale, L. & Pupillo, P. (1997). Dissecting the diphenylene iodonium-sensitive NAD(P)H:quinone oxidoreductase of zucchini plasma membranes. *Plant Physiol.* **114**, 737-46.
64. Steffens, J.C., Lynn, D.G., Kamat, V.S. & Riopel, J.L. (1982). Molecular specificity of haustorial induction in *Agalinis purpurea* (L.) Raf. (Scrophulariaceae). *Ann. Botany* **50**, 1-7.
65. Fry, S. (1983). Ferulated pectins from the primary cell wall: their structure and possible functions. *Planta* **157**, 111-123.
66. Baga, M., Chibbar, R.N. & Kartha, K.K. (1995). Molecular cloning and expression analysis of peroxidase genes from wheat. *Plant Mol. Biol.* **29**, 647-662.
67. Buffard, D., et al., & Esnault, R. (1990). Molecular cloning of complementary DNAs encoding two cationic peroxidases from cultivated peanut cells. *Proc. Natl Acad. Sci. USA.* **87**, 8874-8878.
68. Omann, F., Beaulieu, N. & Tyson, H. (1994). cDNA sequence and tissue-specific expression of an anionic flax peroxidase. *Genome* **37**, 137-147.

69. Mazza, G. & Welinder, K.G. (1980). Covalent structure of turnip peroxidase 7: Cyanogen bromide fragments, complete structure, and comparison to horseradish peroxidase C. *Eur. J. Biochem.* **108**, 481-489.
70. Intaprak, C., Higashimura, N., Yamamoto, K., Okada, N., Shinmyo, A. & Takano, M. (1991). Nucleotide sequences of two genomic DNAs encoding peroxidase of *Arabidopsis thaliana*. *Gene* **98**, 237-241.
71. Intaprak, C., Takano, M. & Shinmyo, A. (1994). Nucleotide sequence of a new cDNA for peroxidase from *Arabidopsis thaliana*. *Plant Physiol.* **104**, 285-286.
72. Fujiyama, K., *et al.* & Okada, H. (1988). Structure of the horseradish peroxidase isozyme c genes. *Eur. J. Biochem.* **173**, 681-687.
73. Diaz-De-Leon, F., Klotz, K.L. & Lagrimini, M. (1993). Nucleotide sequence of the tobacco (*Nicotiana tabacum*) anionic peroxidase gene. *Plant Physiol.* **101**, 1117-1118.
74. Lagrimini, L.M., Burkhart, W., Moyer, M. & Rothstein, S. (1987). Molecular cloning of complementary DNA encoding the lignin forming peroxidase from tobacco: molecular analysis and tissue-specific expression. *Proc. Natl Acad. Sci. USA* **84**, 7542-7546.
75. Kawai, S., Matsumoto, Y., Kajita, S., Yamada, K., Katayama, Y. & Morohoshi, N. (1993). Nucleotide sequence for the genomic DNA encoding an anionic peroxidase gene from a hybrid poplar, *Populus kitakamiensis*. *Biosci. Biotech. Biochem.* **57**, 131-133.
76. Matsumoto, S., Narita, H., Ikura, K & Sakaki, R. (1996). Nucleotide sequence of cationic peroxidases abundantly secreted by cultured tobacco cell. *Plant Physiol.* **110**, 713-714.
77. Botella, M.A., Quesada, M.A., Hasegawa, P.M. & Valpuesta, V. (1993). Nucleotide sequences of two peroxidase genes from tomato (*Lycopersicon esculentum*). *Plant Physiol.* **103**, 665-666.
78. Johansson, A., Rasmussen, S.K., Harthill, J.E. & Welinder, K.G. (1992). cDNA, amino acid and carbohydrate sequence of barley seed-specific peroxidase BP1. *Plant Mol. Biol.* **18**, 1151-1161.